THE CRITICAL ROLE OF THE HISTONE MODIFICATION ENZYME SETDB2 IN THE PATHOGENESIS OF ACUTE RESPIRATORY DISTRESS SYNDROME

Shota Sonobe,[*†] **Masahiro Kitabatake,*** **Atsushi Hara,*** **Makiko Konda,**[*†]
Noriko Ouji-Sageshima,* **Chiyoko Terada-Ikeda,**[‡] **Ryutaro Furukawa,**[*§]
Natsuko Imakita,[*§] **Akihisa Oda,**[∥] **Maiko Takeda,**[‡] **Shiki Takamura,**[¶] **Satoki Inoue**[**]
Steven L. Kunkel,[††] **Masahiko Kawaguchi,**[†] **and Toshihiro Ito***

*Department of Immunology, Nara Medical University, Kashihara, Japan; †Department of Anesthesiology, Nara Medical University, Kashihara, Japan; ‡Department of Diagnostic Pathology, Nara Medical University, Kashihara, Japan; §Center for Infectious Diseases, Nara Medical University, Kashihara, Japan; ∥Department of Pediatrics, Nara Medical University, Kashihara, Japan; ¶Laboratory for Immunological Memory, RIKEN Center for Integrative Medical Sciences, Kanagawa, Japan; **Department of Anesthesiology, Fukushima Medical University, Fukushima, Japan; and ††Department of Pathology, University of Michigan Medical School, Ann Arbor, Michigan

ABSTRACT—**Introduction:** Acute respiratory distress syndrome (ARDS) is a severe hypoxemic respiratory failure with a high in-hospital mortality. However, the molecular mechanisms underlying ARDS remain unclear. Recent findings have indicated that the onset of severe inflammatory diseases, such as sepsis, is regulated by epigenetic changes. We investigated the role of epigenetic changes in ARDS pathogenesis using mouse models and human samples. **Methods:** Acute respiratory distress syndrome was induced in a mouse model (C57BL/6 mice, myeloid cell or vascular endothelial cell [VEC]–specific SET domain bifurcated 2 [Setdb2]–deficient mice [Setdb2^{ff}Lyz2^{Cre+} or Setdb2^{ff}Tie2^{Cre+}], and Cre^{-} littermates) by intratracheal administration of lipopolysaccharide (LPS). Analyses were performed at 6 and 72 h after LPS administration. Sera and lung autopsy specimens from ARDS patients were examined. **Results:** In the murine ARDS model, we observed high expression of the histone modification enzyme *SET domain bifurcated 2* (*Setdb2*) in the lungs. *In situ* hybridization examination of the lungs revealed *Setdb2* expression in macrophages and VECs. The histological score and albumin level of bronchoalveolar lavage fluid were significantly increased in Setdb2^{ff}Tie2^{Cre+} mice following LPS administration compared with Setdb2^{ff}Tie2^{Cre-} mice, whereas there was no significant difference between the control and Setdb2^{ff}Lyz2^{Cre+} mice. Apoptosis of VECs was enhanced in Setdb2^{ff}Tie2^{Cre+} mice. Among the 84 apoptosis-related genes, the expression of *TNF receptor superfamily member 10b* (*Tnfrsf10b*) was significantly higher in Setdb2^{ff}Tie2^{Cre+} mice than in control mice. Acute respiratory distress syndrome patients' serum showed higher SETDB2 levels than those of healthy volunteers. SETDB2 levels were negatively correlated with the partial pressure of oxygen in arterial blood/fraction of inspiratory oxygen concentration ratio. **Conclusion:** Acute respiratory distress syndrome elevates *Setdb2*, apoptosis of VECs, and vascular permeability. Elevation of histone methyltransferase Setdb2 suggests the possibility to histone change and epigenetic modification. Thus, Setdb2 may be a novel therapeutic target for controlling the pathogenesis of ARDS.

KEYWORDS—Epigenetics; acute respiratory distress syndrome; apoptosis; endothelial cell; macrophage; SET domain bifurcated 2

INTRODUCTION

Acute respiratory distress syndrome (ARDS) is a life-threatening disorder clinically characterized by severe hypoxia and bilateral pulmonary infiltrates (1). Sepsis, bacterial and viral pneumonia, and trauma are the leading risk factors for ARDS development (2). Recently, the number of ARDS patients worldwide has dramatically increased owing to the large number of COVID-19 patients (3,4). Currently, no specific therapies are available to reduce the mortality of ARDS; therefore, ARDS remains a deadly syndrome without a specific cure. The pathogenesis of ARDS is characterized by increased permeability of the capillary barrier and influx of protein and inflammatory cell–rich fluid into the alveolar space, leading to hypoxia and lung damage (2). Endothelial cell apoptosis is closely associated with the initiation and progression of ARDS (1,5). Elucidation of the mechanisms underlying ARDS may lead to the development of therapeutic agents and reduce patient mortality.

Previous studies have revealed that the elevation of inflammatory cytokines, called a "cytokine storm," is a hallmark of ARDS, and macrophages play a key role in the pathogenesis of ARDS (6,7). Inflammatory cytokines, such as TNF-α, IL-1β, and IL-6, activate endothelial cells, and the overproduction of these cytokines (cytokine storm) leads to disruption of homeostasis and increased permeability of the capillary barrier (8). Recent studies in models of sepsis and severe inflammatory diseases have suggested that cytokine storms also induce epigenetic changes, such as histone modifications in various promoter regions (9–11). However, little is known about the contribution of epigenetics to ARDS pathogenesis.

We investigated the correlation between epigenetic-related genes and ARDS pathogenesis using an lipopolysaccharide (LPS)-induced lung injury mouse model.

METHODS

Ethics statement

All experiments involving humans in this study were approved by the Ethics Committee of the Nara Medical University (approval no. 2052). All animal experiments performed in this study were approved by the Animal Care and Use Committee at Nara Medical University (approval no. 12958), and all experiments were performed according to the Care and Use of Laboratory Animals at Nara Medical University and ARRIVE (Animal Research: Reporting of *In Vivo* Experiments) guidelines.

Patients

Eleven patients who entered the intensive care unit (ICU) of Nara Medical University Hospital and were diagnosed with ARDS according to the Berlin definition (12) between January 2019 and January 2021 were included in this study. All patients' families provided written informed consent before blood sample collection. The median patient age was 72 years (95% confidence interval, 67–77 years). All the patients underwent ventilatory management. Blood samples were collected daily after the patients entered the ICU for ARDS until day 7 (or ICU exit). Sera were stored at $-80°C$ until enzyme-linked immunosorbent assay (ELISA) was performed. Blood gas analyses were performed daily. Sera were collected from 10 healthy volunteers as controls.

ARDS animal model

C57BL/6 mice (6–8 weeks old) were purchased from CLEA Japan (Tokyo, Japan). Setdb2^{ff} (SET domain bifurcated 2) and myeloid cell–specific Setdb2-deficient mice (Setdb2^{ff}Lyz2^{cre+} mice) were kindly provided by Dr. Steven L. Kunkel (University of Michigan Medical School) (13). Setdb2^{ff} mice were crossed with Tie2-Cre mice (#00863; Jackson Laboratory, Bar Harbor, ME) to generate vascular endothelial cell (VEC)–specific Setdb2-deficient (Setdb2^{ff}Tie2^{cre+}) mice. In this study, we prepared the following four types of transgenic mice: (i) Setdb2^{ff}Lyz2^{cre+} mice (myeloid cell–specific Setdb2-deficient mice), (ii) Setdb2^{ff}Lyz2^{cre-} mice (control mice for Setdb2^{ff}Lyz2^{cre+} mice), (iii) Setdb2^{ff}Tie2^{cre+} mice (VEC-specific Setdb2-deficient mice), and (iv) Setdb2^{ff}Tie2^{cre-} mice (control mice for Setdb2^{ff}Tie2^{cre+} mice). All mice were maintained under specific pathogen-free conditions at the Laboratory Animal Research Center of the Nara Medical University. The male and female mice were housed individually, were allowed food and water *ad libitum*, and were raised in a 12-h light/12-h dark cycle. Mice were anesthetized by i.p. injection of sodium pentobarbital (80 mg/kg) and then inoculated through the upper airway with 2.5 mg/kg LPS (O55:B5; Sigma-Aldrich, St. Louis, MO) diluted in phosphate-buffered saline (PBS; Fujifilm Wako, Osaka, Japan) or 50 μL of PBS for the control group. After 6 or 72 h, the mice were euthanized by collecting blood from the heart under anesthesia. Bronchoalveolar lavage fluid (BALF) was harvested by the direct instillation of 0.7 mL PBS through the trachea. Samples were centrifuged at 800g for 5 min, and supernatants were stored at $-80°C$ until ELISA was performed. Cells in BALF were centrifuged on slides using Cytospin 3 (Thermo Fisher Scientific, Waltham, MA) and stained with modified Wright-Giemsa staining kit (Diff-Quik; Sysmex, Kobe, Japan), Neutrophils and macrophages were counted for each sample by microscopy.

Histological analysis

The left lung lobe was inflated, fixed with 4% paraformaldehyde, and embedded in paraffin. Tissues were sliced into sections (1–2 μm thick), deparaffinized with xylene, and stained with Mayer hematoxylin (Sakura Finetek Japan Co. Ltd., Tokyo, Japan) and eosin (Nacalai Tesque Inc., Kyoto, Japan). The severity of the pneumonia sections was scored (0, absence; 1, mild; 2, moderate; 3, severe) in the following categories: (i) presence of interstitial inflammation, (ii) alveolar inflammation, (iii) pleurisy, (iv) bronchitis, and (v) vasculitis. The final score was calculated as the product of the individual scores. In addition, 1 point was added for pneumonia, edema, and thrombus formation, and 0.5 point was added for infiltration of more than 10% of the lung area (14). A trained pathologist performed blinded histological assessments.

In situ hybridization

Expression of *Setdb2* mRNA was visualized using the ViewRNA ISH Tissue Evaluation Kit (Thermo Fisher Scientific) in accordance with the manufacturer's instructions. Briefly, deparaffinized lung sections were boiled for 10 min and treated with a protease solution for 20 min. After formalin fixation, the ViewRNA TYPE 6 Probe Set (Thermo Fisher Scientific) against *Setdb2* was used for hybridization with the samples for 2 h. Signals were amplified by hybridization with the PreAmplifier Mix and Amplifier mix, which allows specific amplification of the target-specific signal by branched DNA technology, and were then developed using the Label Probe 6-AP with FastBlue substrate.

Immunohistochemical staining

Deparaffinized lung sections were incubated in 0.01 M citrate buffer (pH 6.0) at 105°C for antigen retrieval. To deplete endogenous peroxidase, the slides were treated with 0.3% hydrogen peroxide (Fujifilm Wako) for 10 min and incubated with PBS containing 1% human serum AB (Access Biologicals, Vista, CA), 0.5% skim milk (Fujifilm Wako), and 0.05% Tween 20 (Fujifilm Wako) for 15 min. Immunohistochemical staining of lung autopsy specimens from ARDS and non-ARDS patients for SETDB2 and TNFRSF10B was performed using anti-CLLD8/SETDB2 antibody (ab5517) (Abcam, Cambridge, United Kingdom) and an anti-TRAILR2/TNFRSF10B antibody (NB a-56,618) (Novus Biologicals, Centennial, CO). The reactions were visualized using Histofine Simple Stain MAX-PO(R) and Histofine DAB substrate kit (Nichirei Biosciences, Tokyo, Japan) in accordance with the manufacturer's instructions.

Evaluation of apoptosis

Detection of apoptotic cells in the lungs was performed by the TUNEL (TdT-mediated dUTP nick end labeling) assay using the *In Situ* Apoptosis Detection Kit (Takara Bio, Osaka, Japan) in accordance with the manufacturer's instructions. Deparaffinized sections were treated with proteinase K (20 μg/mL) for 15 min and incubated with 3% H_2O_2 for 5 min to block endogenous peroxidase activity. After washing with PBS, the slides were incubated with TdT enzyme for 1 h at 37°C and then reacted with an anti–fluorescein isothiocyanate antibody conjugated with horseradish peroxidase for 30 min at 37°C. TUNEL staining was developed using 3,3′-diaminobenzidine, tetrahydrochloride, and the samples were counterstained with hematoxylin. The number of TUNEL-positive cells among the VECs was counted using a BZ-X800 optical microscope (Keyence, Osaka, Japan) equipped with software for cell count analysis.

Isolation of lung VECs and macrophages

Mouse lungs were dissociated into single-cell suspensions using a Lung Dissociation Kit (Miltinyi Biotec GmbH, Cologne, Germany) with a gentleMACS Dissociator (Miltinyi Biotec GmbH), according to the manufacturer's instructions. To block Fc receptors, the cells were preincubated with anti-mouse CD16/32 monoclonal antibody (mAb) (BioLegend Inc., San Diego, CA) for 5 min. The cells were then incubated with Alexa Fluor 488–labeled anti-CD11b mAb (BioLegend Inc.), phycoerythrin-labeled anti-CD31 mAb (BioLegend Inc.), phycoerythrin-cyanin 7–labeled anti-CD45 mAb (BioLegend Inc.), or Alexa Fluor 647–labeled anti-F4/80 mAb (BioLegend Inc.) on ice for 30 min. VECs (CD31$^+$CD45$^-$) and macrophages (CD45$^+$CD11b$^+$F4/80$^+$) were sorted using the BD FACS Aria II cell sorter (BD Biosciences, Franklin Lakes, NJ). The data were analyzed using FlowJo software (TreeStar, Ashland, OR). The viability of VECs during flow cytometry was more than 95%, as assessed by 7-amino-actinomycin D staining (BD Biosciences) of CD31$^+$CD45$^-$ cells. The purity of VECs and macrophages was greater than 96%.

RNA extraction and quantitative polymerase chain reaction

Total RNA was extracted from the right lower lobe of the lung using the NucleoSpin RNA kit (Macherey-Nagel GmbH & Co. KG, Düren, Germany). Lung tissues were homogenized with zirconia beads in 700 μL of buffer RA1 containing 1% 2-mercaptoethanol using a bead homogenizer (Wakenyaku Co., Ltd., Kyoto, Japan). Next, 700 μL 70% ethanol was added to each sample. Half of the mixture was added to a NucleoSpin RNA Column and processed according to the manufacturer's instructions. Total RNA was extracted from macrophages and VECs using an RNeasy Micro Kit (Qiagen, Hilden, Germany), in accordance with the manufacturer's instructions. Extracted RNA was reverse-transcribed using Superscript IV Reverse Transcriptase (Thermo Fisher Scientific). Gene expression was analyzed with TaqMan Fast Advanced Master Mix (Thermo Fisher Scientific) using Step One Plus (Thermo Fisher Scientific). TaqMan gene expression assays for *Gapdh* (Mm99999915), *Setdb2* (Mm01318753), *Ncoa3* (Mm00500775), *Smyd1* (Mm00477663), *Hdac9* (01293999), *Birc3* (Mm01168413), *Tnfrsf10b* (Mm00457866), and *Tnfrsf11b* (Mm01205928) were used. Data were analyzed using the relative $^{\Delta\Delta}$CT method and gene expression was normalized to *Gapdh* expression.

Polymerase chain reaction array

Total RNA from whole lungs and isolated lung VECs was reverse transcribed into complementary DNA using an RT^2 First Strand Kit (Qiagen), followed by incubation with reverse transcriptase at 42°C for 15 min followed by incubation at 95°C for 5 min. Complementary DNA was amplified using RT^2 SYBR Green ROX qPCR Mastermix (Qiagen) with the RT^2 Profiler PCR Array Mouse Epigenetic Chromatin Modification Enzyme kit or RT^2 Profiler PCR Array Mouse Apoptosis Enzyme kit (Qiagen), according to the manufacturer's instructions. The results were analyzed using RT^2 Profiler Array Date Analysis v3.5 (Qiagen), and gene expression was normalized to the expression of various housekeeping genes.
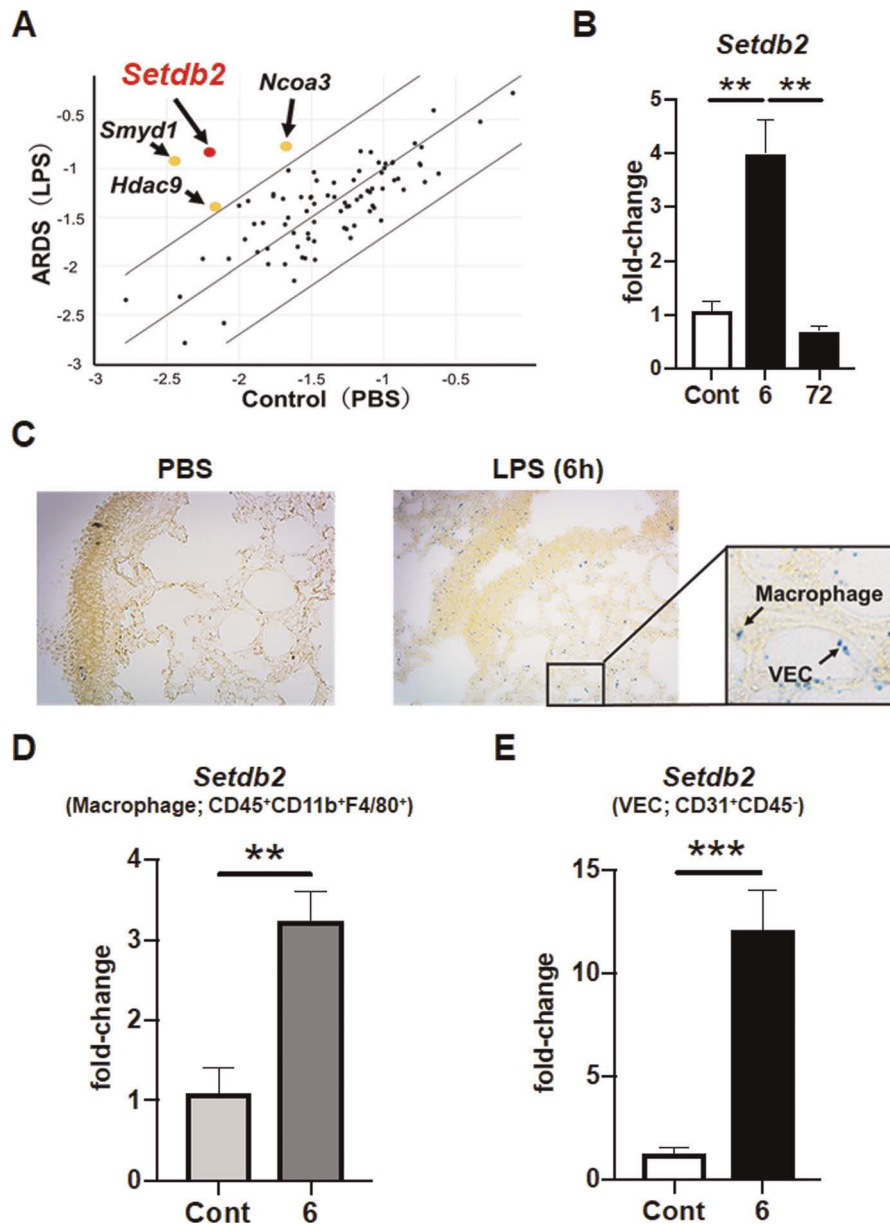
FIG. 1. **Establishment of ARDS model mice and evaluation of *Setdb2* expression in macrophages and lung VECs in mice**. A, The gene expressions of 84 chromatin modification enzymes in whole lungs from ARDS mice at 6 h after LPS instillation and control mice were analyzed by PCR array. The fold regulation threshold was 2. B, The expression levels of *Setdb2* in whole lungs at 6 or 72 h after LPS instillation were analyzed. Data are shown as the mean ± SEM (PBS control, n = 8; 6 h post-LPS, n = 14; 72 h post-LPS, n = 6). C, *In situ* hybridization of *Setdb2* in lung sections: PBS control and 6 h after LPS administration. D, Gene expression of *Setdb2* in lung macrophages at 6 h after LPS administration. Data are shown as the mean ± SEM (PBS control [Cont], n = 3; LPS, n = 6). E, Gene expression of *Setdb2* in lung VECs at 6 h after LPS administration. Data are shown as the mean ± SEM (control, n = 5; LPS, n = 11). **$P < 0.01$, ***$P < 0.001$. ARDS, acute respiratory distress syndrome; PBS, phosphate-buffered saline; PCR, polymerase chain reaction; Setdb2, SET domain bifurcated 2; VECs, vascular endothelial cells.

Enzyme-linked immunosorbent assay

Albumin levels in the BALF of the ARDS mouse model and controls were measured using mouse albumin ELISA Kits (Fujifilm Wako Shibayagi, Gunma, Japan). Human SETDB2 levels were measured using a Human SETDB2 ELISA Kit (MY BioSource, San Diego, CA) in accordance with the manufacturer's instructions.

Statistical analysis

Statistical analyses were performed using Prism 8.0 (GraphPad Software, La Jolla, CA). The Mann-Whitney *U* test or one-way ANOVA was used for comparison. Data are expressed as the mean ± SEM from at least two independent experiments. Spearman correlation coefficient was used to analyze the correlation between SETDB2 activity and the partial pressure of oxygen in arterial blood/

fraction of inspiratory oxygen concentration (PaO$_2$/FIO$_2$) ratio. Statistical significance was set at $P < 0.05$.

RESULTS

Establishment of a murine ARDS model and increased histone modification enzyme expression in ARDS model mice

We established an ARDS mouse model by direct instillation of LPS through the upper airway. In the control group, 50 μL PBS was directly inoculated into the upper airway. Histological analysis revealed the accumulation of leukocytes in the lung parenchyma at 6 h after LPS treatment and dense accumulation of
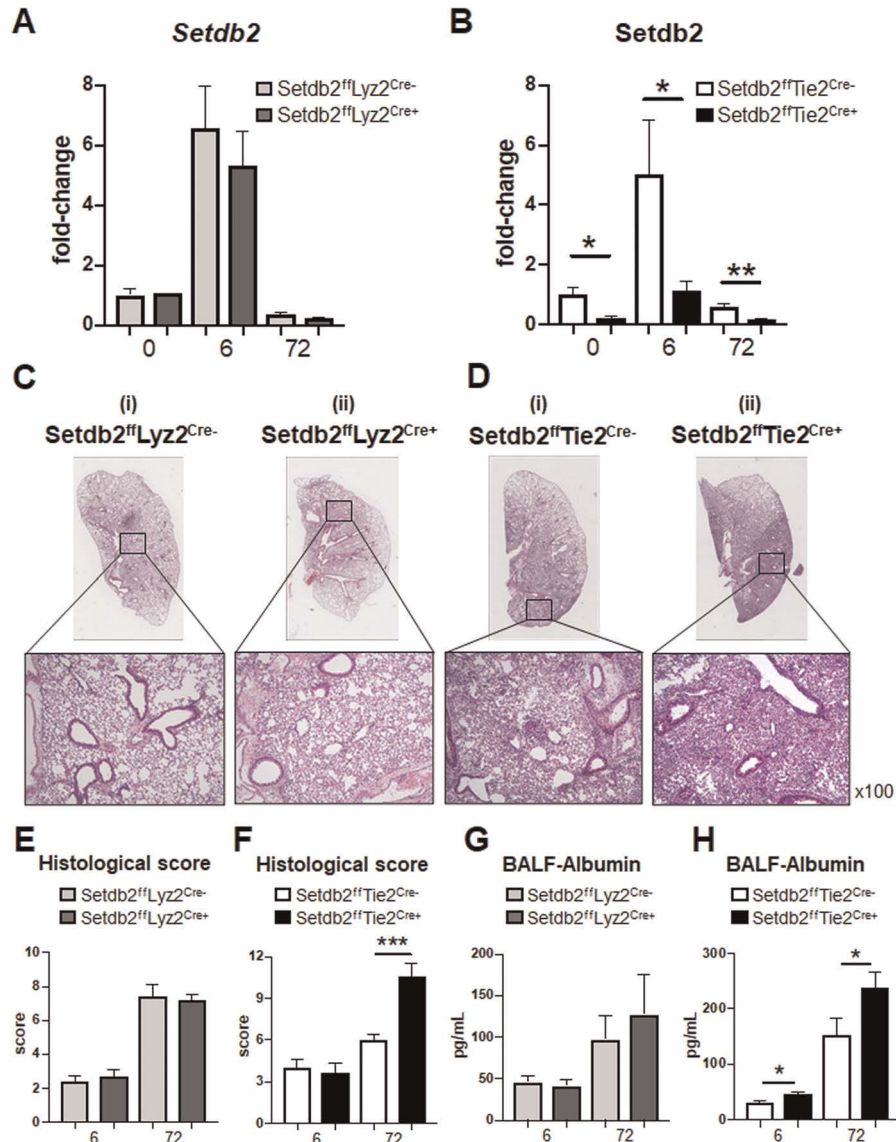
FIG. 2. **Evaluation of ARDS severity in mice with myeloid cell– or VEC-specific knockout of Setdb2.** A and B, Gene expression of *Setdb2* in whole-lung cells from Setdb2ffLyz2cre− mice, Setdb2ffLyz2cre+ mice, Setdb2ffTie2cre− mice, and Setdb2ffTie2cre+ mice at 6 or 72 h after LPS administration. Data are shown as the mean ± SEM. C and D, HE staining of the lungs from 72 h after LPS administration. E and F, Histological scores of lung sections at 6 or 72 h after LPS administration. G and H, Concentration of albumin levels from BALF. Data are shown as the mean ± SEM. 6 h post-LPS: Setdb2ffLyz2cre−, n = 14; Setdb2ffLyz2cre+, n = 11; Setdb2ffTie2cre−, n = 4; Setdb2ffTie2cre+, n = 5; 72 h post-LPS: Setdb2ffLyz2cre−, n = 7; Setdb2ffLyz2cre+, n = 7, Setdb2ffTie2cre−, n = 8; Setdb2ffTie2cre+, n = 11. *$P < 0.05$, **$P < 0.01$, ***$P < 0.001$. ARDS, acute respiratory distress syndrome; BALF, bronchoalveolar lavage fluid; HE, hematoxylin-eosin; Setdb2, SET domain bifurcated 2; VEC, vascular endothelial cells.

leukocytes and pulmonary edema at 72 h, confirming the successful establishment of the ARDS model (Supplemental Fig. 1, http://links.lww.com/SHK/B704).

Next, we examined the association between histone modification enzymes and ARDS pathogenesis. We performed a polymerase chain reaction (PCR) array for genes encoding chromatin modification enzymes in the whole lungs at 6 h after LPS administration. Of the 84 genes tested for chromatin modification enzymes, *SET domain bifurcated 2* (*Setdb2*), *SET and MYND domain-containing 1* (*Smyd1*), *nuclear receptor coactivator 3* (*Ncoa3*), and *histone deacetylase 9* (*Hdac9*) showed markedly higher expression levels in the ARDS group than in the control group (Fig. 1A). Quantitative PCR revealed that the expression of *Setdb2* in whole lungs increased at 6 h after LPS instillation

and returned to basal levels at 72 h (Fig. 1B). In contrast, there was no significant upregulation in *Smyd1*, *Ncoa3*, and *Hdac9* expression at 6 or 72 h after LPS instillation (Supplemental Fig. 2, http://links.lww.com/SHK/B704). Therefore, we selected *Setdb2* for the subsequent analysis.

Next, we examined which cell type expressed *Setdb2* in the ARDS model. *In situ* hybridization of lung sections revealed that *Setdb2* was expressed specifically in macrophages and VECs at 6 h after LPS instillation, whereas *Setdb2* was expressed at low levels in these cell types in the control group (Fig. 1C). We further sorted macrophages (CD45+CD11b+F4/80+) and VECs (CD31+CD45−) from whole lungs at 6 h after the administration of PBS or LPS (Supplemental Fig. 3, http://links.lww.com/SHK/B704) and analyzed *Setdb2* levels in both cell populations.
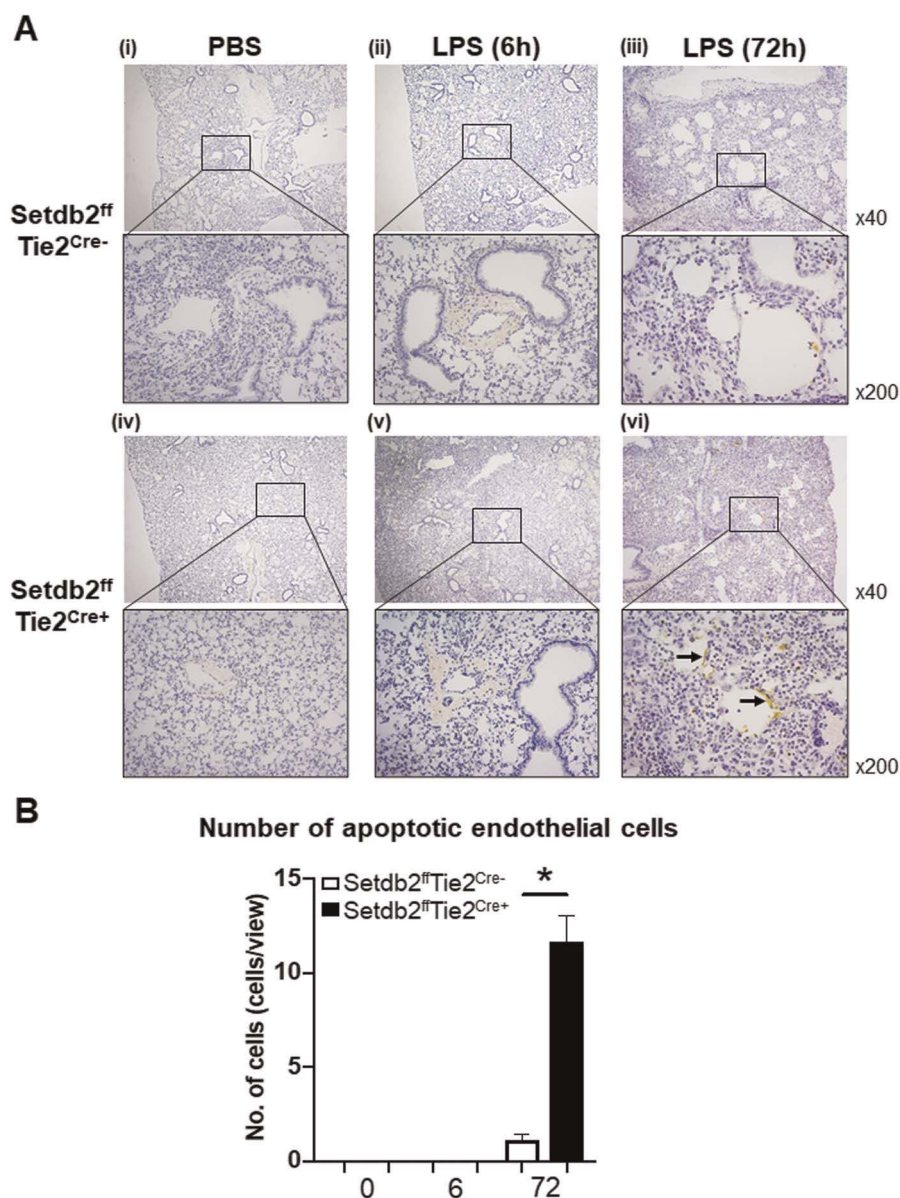
FIG. 3. **Evaluation of apoptosis in lung injury using VEC-specific Setdb2 knockout mice**. Setdb2^{ff}Tie2^{cre-} (n = 7) and Setdb2^{ff}Tie2^{cre+} (n = 6) mice were directly injected with PBS or LPS (2.5 mg/kg) through the upper airway. Mice were killed at 6 or 72 h, and the lungs were harvested. A, Lung sections were stained by TUNEL. Nuclei were stained with hematoxylin. Arrow indicates apoptotic VECs. B, Apoptotic cell count was scored and quantified. n = 3 each group. *$P < 0.05$ versus Setdb2^{ff}VEC^{cre-} mice. PBS, phosphate-buffered saline; Setdb2, SET domain bifurcated 2; TUNEL, TdT-mediated dUTP nick end labeling; VECs, vascular endothelial cells.

Setdb2 expression in both cell populations was significantly increased by LPS instillation compared with that in the control group ($P < 0.01$, $P < 0.001$; Fig. 1, D and E).

Setdb2 knockout in VECs, but not macrophages, exacerbated the pathogenesis of ARDS

To investigate whether Setdb2 in macrophages and/or VECs contributes to ARDS pathogenesis, we generated myeloid cell–specific Setdb2-deficient mice (Setdb2^{ff}Lyz2^{cre+} mice) and VEC-specific Setdb2-deficient mice (Setdb2^{ff}Tie2^{cre+} mice). We examined *Setdb2* expression in the lungs of Setdb2^{ff}Lyz2^{cre+} and Setdb2^{ff}Tie2^{cre+} mice following LPS instillation. There was no significant difference in *Setdb2* expression in whole lungs

between Setdb2^{ff}Lyz2^{cre-} (control) and Setdb2^{ff}Lyz2^{cre+} (knockout) mice, whereas VEC-specific Setdb2-deficient mice (Setdb2^{ff}Tie2^{cre+} mice) showed significantly lower expression of *Setdb2* in whole lungs than Setdb2^{ff}Tie2^{cre-} (control) mice (Fig. 2, A and B). Moreover, histological findings revealed that lung inflammation was similar between Setdb2^{ff}Lyz2^{cre-} (control) and Setdb2^{ff}Lyz2^{cre+} (knockout) mice at both 6 and 72 h after LPS instillation (Supplemental Fig. 4A(i), 4A(ii), http://links.lww.com/SHK/B704, Fig. 2C(i), 2C(ii)), and there were no significant differences in histological score and albumin level in BALF among groups (Fig. 2, E and G). In contrast, lung inflammation in Setdb2^{ff}Tie2^{cre+} mice was more severe than in control mice (Supplemental Fig. 4B(i), 4B(ii), http://links.lww.com/SHK/B704, Fig. 2D(i), 2D(ii)). In
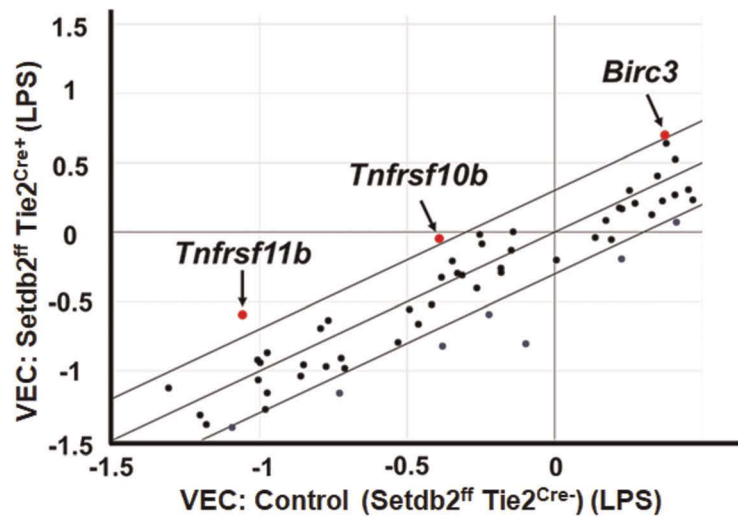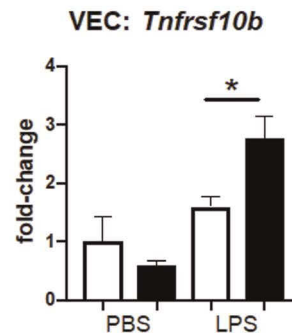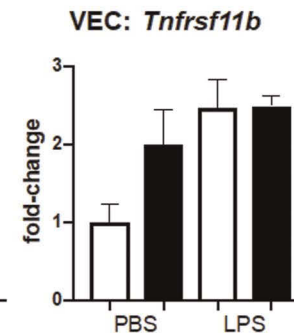
Fig. 4. **Expression of apoptosis-related genes in lung VECs from ARDS model mice**. A, The gene expressions of 84 apoptosis-related genes in lung VECs isolated from Setdb2^{ff}Tie2$^{cre−}$ or Setdb2^{ff}Tie2^{cre+} mice at 6 h after LPS instillation were analyzed by PCR array. The fold regulation threshold was 2. B–D, The expression levels of *Birc3* (B), *Tnfrsf10b* (C), and *Tnfrsf11b* (D) from lung VECs at 6 h after LPS instillation were analyzed. Data are shown as the mean ± SEM (PBS-Setdb2^{ff}Tie2$^{cre−}$, n = 3; PBS-Setdb2^{ff}Tie2^{cre+}, n = 3; LPS-Setdb2^{ff}Tie2$^{cre−}$, n = 7; LPS-Setdb2^{ff}Tie2^{cre+}, n = 6). *$P < 0.05$. ARDS, acute respiratory distress syndrome; PBS, phosphate-buffered saline; PCR, polymerase chain reaction; Setdb2, SET domain bifurcated 2; VECs, vascular endothelial cells.

addition, higher histological scores and significantly increased albumin levels in BALF were observed in Setdb2^{ff}Tie2^{cre+} mice than in control mice (Fig. 2, F and H).

Setdb2 contributes to apoptosis of lung VECs in the ARDS model

We measured inflammatory cytokines in both BALF and parenchyma, but no significant change was observed in Sedb2^{ff}Tie2^{Cre+} mice compared with control mice (Supplemental Fig. 5, http://links.lww.com/SHK/B704). In addition, there was no significant difference in either the number or ratio of leukocytes that had infiltrated the alveolar space (Supplemental Fig. 6, http://links.lww.com/SHK/B704). Apoptosis of VECs has been shown to contribute to the progression of lung injury, with hyperpermeability and loss of endothelial barrier function (15,16). TUNEL staining was performed to detect apoptosis. Apoptosis was mainly detected in VECs 72 h after LPS instillation, but not 6 h after LPS instillation; no apoptotic cells were observed in the PBS control (Fig. 3A). The number of apoptotic cells was significantly higher in Setdb2^{ff}Tie2^{cre+} mice at 72 h after LPS instillation than in control mice (Setdb2^{ff}Tie2$^{cre−}$ mice) (Fig. 3B).

Enhanced apoptosis-related gene levels in VECs from the Setdb2^{ff}Tie2^{cre+} ARDS model

To investigate which apoptosis-related genes were correlated with lung VECs in Setdb2^{ff}Tie2^{cre+} mice during lung injury, we performed a PCR array for genes related to apoptosis in lung VECs at 6 h after LPS instillation. Of the 84 genes tested for apoptosis-related proteins, the expression of *baculoviral IAP repeat-containing protein 3* (*Birc3*), *TNF receptor superfamily member 10b* (*Tnfrsf10b*), and *Tnfrsf11b* was higher in Setdb2^{ff}Tie2^{cre+} mice than in the control (Setdb2^{ff}Tie2$^{cre−}$) group (Fig. 4A). Quantitative PCR of VECs revealed that only *Tnfrsf10b* expression was significantly higher in the Setdb2^{ff}Tie2^{cre+} group than that in the control group; other genes were not significantly upregulated (Fig. 4, B, C, and D).

Elevation of SETDB2 and TNFRSF10B in lung of human ARDS patients

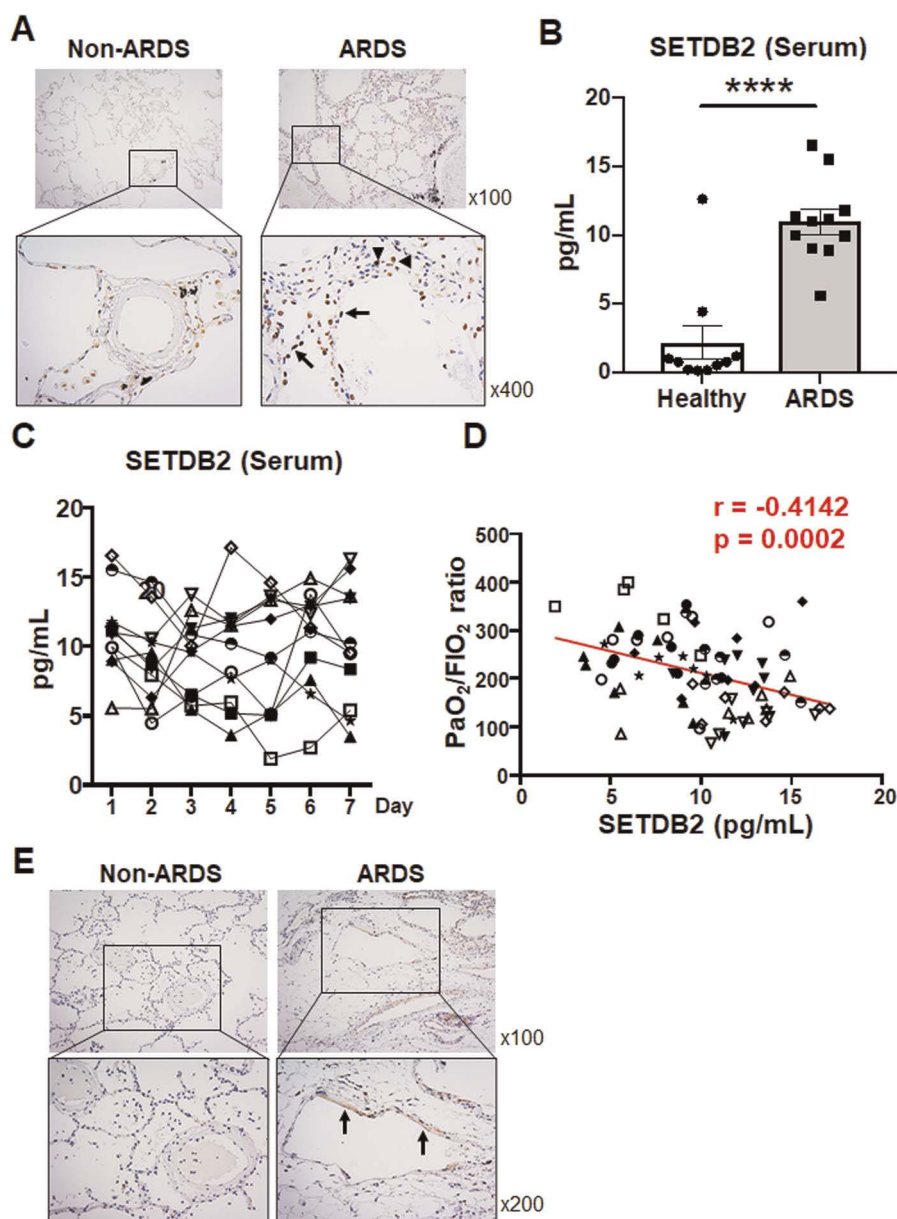To investigate the contribution of SETDB2 to ARDS, we analyzed samples from patients with ARDS. Lung autopsy specimens

FIG. 5. **SETDB2 protein level is elevated in lungs and sera from human ARDS patients**. A, Immunohistochemical staining of SETDB2 in lung from non-ARDS and ARDS patients. Arrowhead shows SETDB2$^+$ VECs, and arrow shows SETDB2$^+$ macrophages. B, Serum SETDB2 protein level from healthy volunteers and ARDS patients at ICU administration (day 1). Data are shown as the mean ± SEM (control, n = 10; ARDS patients, n = 11). ****$P < 0.0001$. C, Change of SETDB2 level in sera from ARDS patients. Each symbol shape represents individual patients. D, The correlation of SETDB2 level in sera with PaO$_2$/FIO$_2$ ratio in all ARDS patient samples (days 1–7). E, Immunohistochemical staining of TNFRSF10B in lung from non-ARDS or ARDS patients. Arrow shows TNFRSF10B$^+$ VECs. ARDS, acute respiratory distress syndrome; ICU, intensive care unit; PaO$_2$/FIO$_2$, partial pressure of oxygen in arterial blood/fraction of inspiratory oxygen concentration; TNFRSF10B, TNF receptor superfamily member 10b; VECs, vascular endothelial cells.

from non-ARDS patients revealed that SETDB2 was expressed mainly in alveolar macrophages, whereas specimens from ARDS patients revealed high SETDB2 levels, especially in VECs and macrophages (Fig. 5A). In addition, serum SETDB2 levels at the time of ICU administration were significantly higher in patients with levels in healthy volunteers (Fig. 5B). High SETDB2 levels persisted for at least 1 week in all 11 ARDS patients (Fig. 5C). Moreover, SETDB2 levels showed a significant inverse correlation with the PaO$_2$/FIO$_2$ ratio (Fig. 5D), an index of oxygenation ability and one of the diagnostic criteria under the Berlin Definition of ARDS. In addition, TNFRSF10B was strongly expressed specifically in VECs of ARDS lung samples (Fig. 5E). Serum

TNFRSF10B levels in sera from both healthy volunteers and patients with ARDS were not detectable by ELISA (data not shown).

DISCUSSION

In this study, we found that the gene expression of the histone modification enzyme Setdb2 was induced in ARDS model mice and ARDS patients. *Setdb2* expression was detected in macrophages and VECs of the lungs. Using myeloid cell–specific and VEC-specific Setdb2 knockout mice, we demonstrated that Setdb2 is involved in the process of ARDS and might be suppressing the worst effects of the LPS injection. VEC–specific

Setdb2 knockout mice showed exacerbated apoptosis of VECs, leading to enhanced lung damage and albumin leakage.

ARDS is a lung disease associated with high mortality and morbidity rates, and no pharmacological interventions are available to reduce mortality. ARDS features, such as noncardiogenic pulmonary edema, are caused by pulmonary microvascular hyperpermeability (2). The mechanisms underlying the onset and exacerbation of ARDS have not been elucidated. Several studies have used LPS as a model of ARDS (17,18). LPS, a major component of the outer membrane of gram-negative bacteria and a ligand for Toll-like receptor 4, induces inflammatory cytokines, such as TNF-α, IL-1β, IL-6, and type I interferons (IFNs), and is a cause of sepsis (19). Therefore, we selected the LPS-induced ARDS model for this study. Setdb2 is reportedly induced by type I IFNs (20). LPS stimulation through Toll-like receptor 4 induces IFN-β by the Toll/IL-1R domain-containing adaptor, inducing the IFN-β−dependent pathway (21), suggesting that the expression of Setdb2 is induced *via* this signaling pathway.

Several studies have reported changes in gene expression, including inflammatory cytokine genes, in ARDS mouse models (22). Epigenetic mechanisms, particularly histone modifications, positively or negatively modulate inflammatory responses, depending on the modification (23). For example, H3K4 methylation, which is associated with active transcription, induces inflammation, whereas H3K27 methylation, which is associated with transcriptional repression, inhibits the inflammatory response (24). Of the 84 histone modification enzymes examined in this study, Setdb2 was the only enzyme that was elevated in the lungs of the ARDS model. A previous report indicated that Setdb2, a histone methyltransferase that suppresses target gene expression by methylating H3K9 (25), regulates monocyte- and macrophage-mediated immunity in a severe inflammation model of influenza virus pneumonia (13). Thus, we hypothesized that Setdb2 in macrophages may be responsible for acute lung inflammation in ARDS and generated a myeloid cell–specific Setdb2 knockout mouse model (Setdb2[ff]Lyz2[cre+] mice). However, there were no differences in inflammatory cytokine levels (data not shown), lung histological changes, vascular permeability, or other physiological findings between Setdb2[ff]Lyz2[cre+] and control mice. We did not find any exacerbation of ARDS in Setdb2[ff]Lyz2[cre+] mice; however, Setdb2 may have a different function in parenchymal and myeloid-derived cells. Further research is required to elucidate the role of Setdb2 in myeloid cells.

VECs play a central role in the mechanism underlying fluid leakage to the alveoli in ARDS, and the disruption of VECs is regarded as a hallmark of ARDS (16). We have previously reported high *Setdb2* expression in brain VECs in a murine influenza-associated encephalopathy model (26). Moreover, previous studies have shown that apoptotic signals alter vascular permeability, contributing to hyperpermeability (27,28). We found that the number of apoptotic VECs was significantly higher in Setdb2[ff]Tie2[cre+] mice than in control mice. These results suggest that Setdb2 in VECs, not myeloid cells, including macrophages, contributes to the pathogenesis of ARDS by influencing the apoptosis of lung VECs. The inhibition of murine pulmonary microvascular endothelial cell apoptosis promotes the recovery

of barrier function under septic conditions (29). We also found that *Tnfrsf10b* expression in VECs was increased in Setdb2[ff]Tie2[cre+] mice compared with that in control mice following LPS instillation. *Tnfrsf10b* encodes a TNF receptor superfamily protein that binds TNF-related apoptosis-inducing ligands to mediate apoptosis (30,31) and is expressed in many organs and cells in humans, such as the brain, heart myocytes, alveolar septa, and bronchial epithelium (32). Some studies have reported that Tnfrsf10b is associated with endothelial cell apoptosis (33,34). Whether Setdb2 regulates the *Tnfrsf10b* promoter and the detailed mechanism by which epigenetic changes induced by Setdb2 regulate permeability in ARDS pathogenesis remains unclear. Furthermore, it is unknown whether overexpression of Setdb2 would attenuate the effects of LPS injection.

We further demonstrated that SETDB2 levels in the lungs and sera of patients with ARDS were higher than those in healthy volunteers. Moreover, SETDB2 levels showed a negative correlation with the PaO$_2$/FIO$_2$ ratio, a widely used clinical indicator of hypoxemia, suggesting that Setdb2 may be a marker for ARDS severity and may inhibit apoptosis to prevent the exacerbation of ARDS pathogenesis. SETDB2 has been found to play an important role in regulating inflammation in previous studies (20,35), suggesting that it may be strongly expressed in the regulation of inflammation in the presence of severe inflammatory diseases, such as ARDS. However, the significance of SETDB2 in patients with ARDS and the underlying mechanisms should be further investigated.

In summary, these results demonstrated that Setdb2 plays an indispensable role in the regulation of ARDS. A better understanding of the relationship between epigenetic changes, particularly *via* Setdb2, in VECs during ARDS may provide mechanistic approaches for controlling and modifying the endothelial response during ARDS.

ACKNOWLEDGMENTS

REFERENCES

1. Chambers E, Rounds S, Lu Q: Pulmonary endothelial cell apoptosis in emphysema and acute lung injury. *Adv Anat Embryol Cell Biol* 228:63–86, 2018.
2. Thompson BT, Chambers RC, Liu KD: Acute respiratory distress syndrome. *N Engl J Med* 377:562–572, 2017.
3. Berlin DA, Gulick RM, Martinez FJ: Severe COVID-19. *N Engl J Med* 383:2451–2460, 2020.
4. Li X, Ma X: Acute respiratory failure in COVID-19: is it "typical" ARDS? *Crit Care* 24:198, 2020.
5. Huppert LA, Matthay MA, Ware LB: Pathogenesis of acute respiratory distress syndrome. *Semin Respir Crit Care Med* 40:31–39, 2019.
6. Lomas-Neira J, Chung CS, Perl M, Gregory S, Biffl W, Ayala A: Role of alveolar macrophage and migrating neutrophils in hemorrhage-induced priming for ALI subsequent to septic challenge. *Am J Physiol Lung Cell Mol Physiol* 290: L51–L58, 2006.
7. Johnston LK, Rims CR, Gill SE, McGuire JK, Manicone AM: Pulmonary macrophage subpopulations in the induction and resolution of acute lung injury. *Am J Respir Cell Mol Biol* 47:417–426, 2012.
8. Ye Q, Wang B, Mao J: The pathogenesis and treatment of the 'cytokine storm' in COVID-19. *J Infect* 80:607–613, 2020.

9. Hachiya R, Shiihashi T, Shirakawa I, et al: The H3K9 methyltransferase Setdb1 regulates TLR4-mediated inflammatory responses in macrophages. *Sci Rep* 6:28845, 2016.

10. Carson WF, Cavassani KA, Ito T, et al: Impaired CD4$^+$ T-cell proliferation and effector function correlates with repressive histone methylation events in a mouse model of severe sepsis. *Eur J Immunol* 40:998–1010, 2010.

11. Wei J, Dong S, Bowser RK, et al: Regulation of the ubiquitylation and deubiquitylation of CREB-binding protein modulates histone acetylation and lung inflammation. *Sci Signal* 10:eaak9660, 2017.

12. Ranieri VM, Rubenfeld GD, Thompson BT, et al: Acute respiratory distress syndrome: the Berlin definition. *JAMA* 307:2526–2533, 2012.

13. Kroetz DN, Allen RM, Schaller MA, et al: Type I interferon induced epigenetic regulation of macrophages suppresses innate and adaptive immunity in acute respiratory viral infection. *PLoS Pathog* 11:e1005338, 2015.

14. Schliehe C, Flynn EK, Vilagos B, et al: The methyltransferase Setdb2 mediates virus-induced susceptibility to bacterial superinfection. *Nat Immunol* 16:67–74, 2015.

15. Li X, Shu R, Filippatos G, Uhal BD: Apoptosis in lung injury and remodeling. *J Appl Physiol* 97:1535–1542, 2004.

16. Gill SE, Rohan M, Mehta S: Role of pulmonary microvascular endothelial cell apoptosis in murine sepsis-induced lung injury *in vivo*. *Respir Res* 16:109, 2015.

17. Chen H, Bai C, Wang X: The value of the lipopolysaccharide-induced acute lung injury model in respiratory medicine. *Expert Rev Respir Med* 4:773–783, 2010.

18. Xu Y, Ito T, Fushimi S, et al: Spred-2 deficiency exacerbates lipopolysaccharide-induced acute lung inflammation in mice. *PloS One* 9:e108914, 2014.

19. Kuzmich NN, Sivak KV, Chubarev VN, Porozov YB, Savateeva-Lyubimova TN, Peri F: TLR4 signaling pathway modulators as potential therapeutics in inflammation and sepsis. *Vaccines (Basel)* 5:34, 2017.

20. Kimball AS, Davis FM, denDekker A, et al: The histone methyltransferase Setdb2 modulates macrophage phenotype and uric acid production in diabetic wound repair. *Immunity* 51:258–271, 2019.

21. Yamamoto M, Sato S, Hemmi H, et al: TRAM is specifically involved in the Toll-like receptor 4–mediated MyD88-independent signaling pathway. *Nat Immunol* 4(11):1144–1150, 2003.

22. Lin X, Dean DA: Gene therapy for ALI/ARDS. *Crit Care Clin* 27:705–718, 2011.

23. Medzhitov R, Horng T: Transcriptional control of the inflammatory response. *Nat Rev Immunol* 9:692–703, 2009.

24. Francis M, Gopinathan G, Foyle D, et al: Histone methylation: Achilles heel and powerful mediator of periodontal homeostasis. *J Dent Res* 99:1332–1340, 2020.

25. Rao VK, Pal A, Taneja R: A drive in SUVs: from development to disease. *Epigenetics* 12:177–186, 2017.

26. Imakita N, Kitabatake M, Ouji-Sageshima N, et al: Abrogated caveolin-1 expression *via* histone modification enzyme Setdb2 regulates brain edema in a mouse model of influenza-associated encephalopathy. *Sci Rep* 9:284, 2019.

27. Sagawa N, Oshima Y, Hiratsuka T, et al: Role of increased vascular permeability in chemotherapy-induced alopecia. *In vivo* imaging of the hair follicular microenvironment in mice. *Cancer Sci* 111:2146–2155, 2020.

28. Damarla M, Parniani AR, Johnston L, et al: Mitogen-activated protein kinase–activated protein kinase 2 mediates apoptosis during lung vascular permeability by regulating movement of cleaved caspase 3. *Am J Respir Cell Mol Biol* 50:932–941, 2014.

29. Wang L, Mehta S, Brock M, Gill SE: Inhibition of murine pulmonary microvascular endothelial cell apoptosis promotes recovery of barrier function under septic conditions. *Mediators Inflamm* 2017:3415380–3415315, 2017.

30. Chaudhary PM, Eby M, Jasmin A, Bookwalter A, Murray J, Hood L: Death receptor 5, a new member of the TNFR family, and DR4 induce FADD-dependent apoptosis and activate the NF-kappaB pathway. *Immunity* 7:821–830, 1997.

31. Tanaka F, Kawakami A, Tamai M, et al: IFN-gamma/JAK/STAT pathway–induced inhibition of DR4 and DR5 expression on endothelial cells is cancelled by cycloheximide-sensitive mechanism: novel finding of cycloheximide-regulating death receptor expression. *Int J Mol Med* 15:833–839, 2005.

32. Spierings DC, de Vries EG, Vellenga E, et al: Tissue distribution of the death ligand TRAIL and its receptors. *J Histochem Cytochem* 52:821–831, 2004.

33. Perrot-Applanat M, Vacher S, Toullec A, et al: Similar NF-κB gene signatures in TNF-α treated human endothelial cells and breast tumor biopsies. *PLoS One* 6:e21589, 2011.

34. Fossati S, Ghiso J, Rostagno A: TRAIL death receptors DR4 and DR5 mediate cerebral microvascular endothelial cell apoptosis induced by oligomeric Alzheimer's Aβ. *Cell Death Dis* 3:e321, 2012.

35. Melvin WJ, Audu CO, Davis FM, et al: Coronavirus induces diabetic macrophage–mediated inflammation *via* SETDB2. *Proc Natl Acad Sci U S A* 118(38):e2101071118, 2021.